Toxicology Research

Accepted Manuscript

ROYAL SOCIETY OF CHEMISTRY

www.rsc.org/toxicology

Title: N-ethyl-N- nitrosourea induced transplacental lung tumor development and its control: Molecular modulations for tumor susceptibility in a mouse model. *

Authors: Satya Sahay, Daya S. Upadhyay ** and Krishna P. Gupta***

* **CSIR- IITR Communication No.** 3130

Running Title: Prevention of Transplacental Tumorigenesis

Affiliation & Environmental Carcinogenesis

Address: CSIR-Indian Institute of Toxicology Research

Mahatma Gandhi Marg, Lucknow –226001, India

** Laboratory Animals Services, CSIR-Central Drug Research Institute,

Sitapur Road, Lucknow

*** **Correspondence:** Krishna P. Gupta, PhD.

Email: krishnag522@yahoo.co.in

Tel: +91-522-2627586, Ext.313

Fax: +91-522-2628227

ABSTRACT

Development of lung tumors after transplacental N-ethyl-N- nitrosourea (ENU) exposure has been demonstrated in Swiss and Balb/c mice F1 mice. We also suggest the molecular changes that could be affecting the susceptibility to chemical carcinogens during the tumor development in the fetus. In this study, ENU administered on 17th days of gestation resulted in the formation of lung tumor in Balb/c F1 mice while only lymphocytic infiltration was observed in Swiss F1 mice at the end of three months. Molecular changes were observed in both the strains, but the degree of alterations in some of the genes was more in Balb/c F1 mice as compared to Swiss F1 mice. Administration of 2% inositol hexaphosphate (IP6) to F1 mice attenuated the proliferation, inflammation and up regulated the apoptotic machinery in terms of the expression of cyclin D1, NF-κβ p50, COX-2, mut p53, Bax, Bcl-2, Bcl-$_{XL}$ including caspase enzyme activities and DNA damage. These could be the important pathways involved in the lung tumor development in the offspring from the carcinogen predisposed mothers and IP6 attenuated the lymphocytic infiltration and tumor development by modulating these events. Analysis of molecular changes and the chemopreventive potential of IP6 during ENU induced transplacental lung tumorigenesis suggest, that susceptibility for the induction of lung tumor in Balb/c F1 mice could possibly be due to the greater over expression of genes involved in proliferation, inflammation in the transplacental lung tumor development in Balb/c F1 mice rather than Swiss F1 mice.

KEYWORDS: Swiss; Balb/c; F1 generation; Lung Tumors; ENU; Inositol Hexaphosphate; Apoptosis.

INTRODUCTION

Several studies have shown that the developing organism is very sensitive to chemical and physical carcinogens suggesting that exposure of pregnant women to environmental toxicants may place the embryo and fetus at higher risk for the development of cancer. Also, the different strains of mice exhibit differential susceptibility to both spontaneous and chemically induced transplacental lung tumorigenesis due to interaction between genetic factors and environmental agents that affect the phases of tumorigenesis [1]. Epidemiological and laboratory animal model studies have demonstrated that smoking and exposure of environmental carcinogens to pregnant women could result in the development of cancer in their offspring's [2]. Development of childhood tumors due to the exposure to mothers is alarming and there is need to explore and understand the basis of transplacental tumor development for its management [3].

ENU, a mutagen pertains to the family of N-nitroso compounds (NOCs) that are present in tobacco smoke, fumigants and biohazard that may affect human health [4]. Application of ENU has been used in experimental models during the gestation period to study the transplacental lung carcinogenesis [5, 6]. The testing of mice with ENU serves the similar purpose to estimate the risk or effects associated with mutagens and carcinogens in the human population [7].

The outcome of the study using mouse model could be extrapolated to the situations in human as certain mutations described in mouse lung tumors and the histology are similar to that of human lung cancer [8, 9].

Over expression of cyclin D1, a regulator of cell cycle progression from G1 to S phase, has been linked to the development and progression of lung and other cancers [10]. Up regulation of transcription factor Nf-κβ, a dimmer of p50 and RelA (p65), enhances cell survival by transcribing the cell cycle regulator, cyclin D1 and is considered a molecular link between chronic inflammation and tumor development [11] as it is activated in many types of cancer [12, 13].

Over expression of cyclooxygenase-2 (COX-2) was seen in approximately 70% of lung adenocarcinoma and was associated with cell proliferation, chronic inflammation and resistance to apoptosis [14, 15]. p53, the tumor suppressor gene, is an important defense against cancer as it suppresses tumor growth through cell cycle regulation and also via apoptosis [16-18]. Mutations in the p53 gene facilitate the development of resistance to apoptosis and increased survival of the damaged cells. Up regulation of Bax and down regulation of Bcl-$_{XL}$ and Bcl-2 lead to the activation of key executioner of apoptosis, caspase-3 and caspase-9 [19,20] have been well documented in a p53-dependent pathway [21].

There is an immense need to develop newer therapeutic strategies to improve the lung cancer for better management. The molecular modulations during the tumor development need to be responsive to antitumor agents for their better use as a target for the therapy. Inositol hexaphosphate (IP6), a naturally occurring polyphosphorylated carbohydrate, is present in edibles like rice, grains fruits and vegetables. A substantial amount of IP6 (0.01-1mM) is

present in mammalian cells and exerts its effect after getting converted into lower phosphates [22-25]. It is reported that IP6 can inhibit many types of cancer in different experimental models including prostate, skin, mammary, colon, lung and liver [26-30]. IP6 has been shown to reduce tumor volume, tumor weight, cell proliferation, angiogenesis and induce the apoptosis [25, 31, 32] but molecular mechanisms needs to be explored.

We are showing the ENU induced transplacental lung tumorigenesis in F1 mice in the presence or absence of IP6 and its underlying basis with the emphasis on the representatives of critical pathways involved in tumorigenesis by assessing cyclin D1, Nf-κβp50, COX-2, mut p53 and the balance between pro-apoptotic events such as Bax, caspase-3, caspase-9 and anti-apoptotic events namely, Bcl-2, Bcl-$_{XL}$ in mouse lungs. Chemopreventive agents could inhibit Nf-κβ activation and block the Nf-κβ signaling cascade [33]. Our results would help in better understanding of the mechanisms of transplacental tumor development and the management of the disease by IP6 with the novel molecular basis and the role of IP6 in the lung tumor development and susceptibility in the progeny of exposed mothers.

MATERIAL AND METHODS

Animals

Female Swiss and Balb/c mice (6-8 weeks old and 18-22 gm body weight) from the inbred colony of CSIR-IITR, Lucknow, were used throughout the study. Male Swiss and Balb/c mice were used only for mating. All the animals were kept in 12 h light and dark cycle and given a pellet diet and water ad libitum. This pellet diet consisting of 21.53 % protein; 5.24% fat, 5.3% crude fiber; 57.59% carbohydrate and 363.64 kcal/100g caloric value was procured from M/S Ashirwad Pvt. Ltd., Chandigarh, India.

The study was approved by and the animals were handled according to the norms of the Institutional Animal Ethics Committee (IAEC).

Chemicals

N-ethyl-N-nitrosourea and inositol hexaphosphate were procured from Sigma Chemical Co. USA. AMV-RT-PCR kits, Taq DNA polymerase, dNTPs, PCR primers, bovine serum albumin (BSA) were from Bangalore Genei, India. Enzyme activity assay kits for caspase-3 (Cat no. BF3100) and for caspase-9 (Cat no. BF10100) were procured from R&D systems, USA. Primary rabbit polyclonal COX-2 and Bcl-2 antibodies were purchased from Alexis Biochemicals, USA; rabbit polyclonal Bcl-$_{XL}$, Bax, Nf-κβp50 or cyclin D1 and goat polyclonal caspasae-3 antibodies were purchased from Santa Cruz Biotechnology, USA; mouse polyclonal mut p53 antibody was purchased from Boehringer Mannheim, Germany

and rabbit polyclonal caspase-9 antibody was purchased from Cell Signaling Technology, USA. IgG, HRP-conjugated anti-rabbit, anti-mouse, anti-goat secondary antibodies were obtained from Bangalore Genei, India. The rest of the chemicals were procured from local commercial sources and were of analytical grade.

Chronic Animal Bioassay

Mating was initiated for both the Swiss and Balb/c strains by placing one male with two female mice for a night. Day zero of pregnancy was determined by checking the presence of a vaginal sperm plug next morning. Thereafter, following impregnation, mice (twelve no.) were housed individually. Pregnant mice (six no.) received only 50mM citrate buffer pH 6.0 and another set of pregnant mice (six no.) received ENU i.p.at a dose of 40 mg/kg body weight in 50mM citrate buffer pH 6.0 on the 17^{th} day of gestation. Pups (litter size 4-8/dam; body weight 1-1.5 gram/pup) were delivered after the 18^{th} day of gestation and weaning of the pups was done at the age of 24 days. Untreated pups were further divided into two groups, 1 and2 .Group -1 pups (control) were put on normal drinking water and group-2 pups (IP6) were put on 2% IP6 in drinking water. Pups from the ENU treated mothers were also divided into two groups, 3 and 4. Group -3 pups (ENU) received normal drinking water and group-4 pups (ENU+IP6) received 2% IP6 in drinking water. Treatment details are given in table-1. Dose selection of ENU was based on ours and others earlier reports [3, 34] and the IP6 dose was also based on earlier reports [31, 32, 34]. Considering that mouse drinks an average around 5ml of water, each animal consumed around 100 mg of IP6 in a day.

Swiss and Balb/c F1 mice (body weight 23-30 g/mouse) from each group were sacrificed by cervical dislocation at the end of three months after ENU exposure. The lungs were harvested and tumors on the surface of the lung counted and their sizes determined under a dissecting microscope. Lungs from one third of the mice from each group were fixed in 10% phosphate buffered formalin and lungs from the rest of the mice were taken out and processed for molecular studies.

Histopathological Analysis

Formalin fixed lung tissues were dehydrated in ascending concentrations of ethanol, cleared in xylene, and embedded in paraffin to prepare the blocks. All five lobes of the lungs were sectioned, mounted on slides and stained. The 5 micron serial sections were stained with hematoxylin–eosin and were examined using Leica DFC 295 camera under Leica DM 1000 microscope at the magnification of 40X for histopathological evaluation and counting the tumors. The diameter of the largest section of each tumor was measured using the Leica Live Measurement Software and the area of tumor was calculated in terms of mm^2 [11].

Reverse Transcription Polymerase Chain Reaction (RT-PCR)

Total RNA was isolated using TRIzol (Invitrogen, USA) as per manufacturer's instructions. RNA was treated with DNaseI (Ambion Co. USA) to remove DNA contamination, if any. cDNA was synthesized by RT-PCR using AMV-RT kit as per instructions. cDNA (1 µl) was used as a template for amplification using mRNA Specific primers for specific genes. Nucleotide sequences (MWG, Biotech, Germany) for a gene specific primer are listed in

table-2. PCR was performed after denaturation at 95ºC for 5min, 35 cycles (95ºC for 60s, annealing for the 60s, and amplification at 72ºC for 60s) followed by a final extension for 4 min at 72ºC. PCR products were resolved on 1.5% agarose gel and visualized using ethidium bromide. Quantification was done using Gene Tool Synegene software [11].

Western Blot Analysis of Proteins

The lung tissue extract was prepared in 20mM Tris buffer (pH 7.5) consisting of 2mM sucrose, 2mM EDTA, 0.5mM EGTA, 2mM $MgCl_2$, 2mM PMSF, 1mM DTT, 0.03mM Na_3VO_4 and protease inhibitor cocktail (Sigma Chemical Co. USA). An aliquot equivalent to 50 µg proteins was subjected to SDS PAGE on 10-12.5% Tris-glycine gel. The separated proteins were then transferred onto Immobilion-P-membrane (PVDF) (Millipore, USA) and were probed with COX-2, Bcl-2, Bcl-$_{XL}$, Bax, Nf-κβp50, cyclin D1, caspasae-3, mut p53 or caspase-9 antibody in 5% nonfat milk powder in TBST (100mM Tris–HCl and 150mM NaCl and 0.1% Tween-20) at a dilution of 1:2000 along with peroxidase-conjugated appropriate secondary antibody (Bangalore Genie, India). Signals were visualized using Chemolumiescence HRP detection systems (Millipore, USA) [11] and quantified on Versa Doc (Bio-Rad). Membranes were stripped for reprobing with antibody for β-actin (Sigma Co).

Estimation of Enzyme Activity of Caspase-3 and Caspase-9

The lung tissue extract was prepared in the lysis buffer provided in the caspase assay kit. A 10,000 g supernatant was used to determine the caspase activities using colorimetric protease assay kit that included specific substrates for caspases-3 and -9 according to the

manufacturer's instructions. Briefly, in a 96-well plate, tissue lysate equivalent to 100µg protein in 50µl was added to 50µl 2X reaction buffer containing 10mM DTT and 5 µl of 4mM substrate DEVD-pNA for caspase-3 or LEHD-pNA for caspase-9 (provided with the kit) followed by the incubated at 37ºC for 2h . At the end, absorbance was measured at 405nm in a micro plate reader (BMG Labtech ,USA) [24]. Caspase activity was expressed in terms of optical density /mg protein/hr in figures.

TUNEL Assay

This assay was based on the identification of DNA fragmentation, a hallmark of apoptosis; by terminal deoxynucleotidyl transferase-mediated dUTP nick end-labeling (TUNEL). The procedure was performed using a TACS 2TdT DAB kit (Trevigen, USA,) as per manufacturer's protocol [35]. After deparaffinized, rehydrated in descending concentrations of ethanol (100%, 90%, and 70%). TUNEL positive signals were visualized using the horseradish peroxidase-mediated diaminobenzidine (DAB) staining solution reaction. Cell nuclei were counterstained with a methyl green solution. Then dehydration in ascending concentration of ethanol (70%, 90%, and 100%) followed by DPX mounting.

Protein estimations were done by Bradford reagent (Bio-Rad Laboratories, Inc.USA) using BSA as standard.

Statistical Analysis

Data were expressed as mean value ± SD.Student's't' test was used to analyze the difference in tumors between ENU and ENU+IP6 treated groups. Statistical analysis of the gene expression was performed using the Graph Pad Prism (version 5.0, Graph Pad Software Inc., USA). ANOVA was performed for comparing mean between groups and statistical significance was determined in terms of '*p*' values. Newman–Keuls test analysis was done to compare significant changes among all the groups.

RESULTS

Transplacental lung tumor development in F1 mice

We evaluated tumor development by gross and microscopic examination at the end of three months after single ENU administered on day 17th gestation and found that adult Balb/c F1 mice are more susceptible to tumor induction as compared to Swiss mice.

Gross examination:

No tumor was observed on the lung surface of Swiss F1 mice. While tumors were observed clearly on the lung surface in 12 out of 15 Balb/c F1 mice at the end of 3 months after ENU exposure (Figure 1-I). Total number of visible lung tumors (multiplicity) was 92 in 12 tumor bearing mice. In the presence of 2% IP6, 15 out of 18 mice developed tumors and total number of tumors was 65. There was a reduction in the average number of tumors from 7.6 to 4.3 resulting into 44% inhibition of tumor development in the presence of IP6 (Figure 1-I). There was no effect of ENU on the number of litters and body or lung weight in F1 mice also remained unaffected.

Microscopic Examination of Lung Tumor in Wax Embedded Lung Sections:

Microscopic examination of the lungs was done in F1 mice from both the strains. We did not observe any tumor in Swiss F1 mice from ENU exposed mothers, but some lymphocytic infiltration was observed in one third mice used for the microscopic examination. This lymphocytic infiltration was attenuated by IP6 administration (Figure 1-II). Microscopic evaluation for Balb/c strain was done in 5 F1 mice from ENU exposed group and 6 F1 mice

from ENU treated group drinking 2% IP6. At the end of 3 months, clearly visible defined adenomas were observed in 3 Balb/c F1 mice (Figure 1-III). Total number of tumors in tumor bearing F1 mice from the ENU exposed Balb/c mothers was 23 with an average of 7.6 tumors / tumor bearing mouse . In the presence of 2% IP6, this number was reduced to 10 in 3 in tumor bearing F1 mice with an average of 3.33 tumors / tumor bearing F1 mouse resulting in 57% reduction in tumor development ($p<0.05$) (Figure 1- III). As per the area of the largest section of each tumor, 60% inhibitory effect of IP6 was observed in the size of tumors ($p<0.01$). Tumors size ranged between 0.231 -0.685 mm^2 with an average area of 0.452 mm^2. Tumor size was reduced to the range between 0.020 – 0.390 mm^2 with an average of 0.181 mm^2 tumor area in mice receiving 2% IP6 (Figure 1-III).There were no lung adenomas in the IP6 alone group. Citrate buffer was used as vehicle and no visible effect was observed in Swiss or Balb/c F1 mice.

Status of Proliferation and Inflammation Associated Genes

In order to find the genes responsible for the tumor susceptibility, we tried to evaluate the transplacental effect of ENU on the expression of critically important representative gens of proliferation and inflammation in both Swiss and Balb/c F1 mice**.** Cyclin D1, Nf-κβp50 and COX-2 were found to be upregulated by ENU exposure (Figure 2). The upregulation in mRNA of cyclin D1, Nf-κβ p50 and COX-2 was 37, 24 and 32% in Swiss F1 and 79, 36 and 40% in Balb/c F1 mice with respect to control. In the presence of IP6, the ENU caused mRNA increase was 16, 15 and 14% in Swiss F1 and 55, 0 and 25% in Balb/c F1 with respect to control (Figure 2-I).

The increase in the levels of cyclin D1, Nf-κβ p50 or COX-2 protein was 89, 56 or 36% in Swiss F1 mice .Whereas, in Balb/c F1 mice, the increase for respective genes was 200, 141 or 40% with respect to control. In presence of 2% IP6, the ENU caused increase was attenuated for the respective genes but remained 55, 43 or 20% in Swiss F1 and 29, 84 or 9% in Balb/c F1 mice with respect to control (Figure 2-III).

Modulation of Apoptotic Genes

Various pro- and anti-apoptotic proteins play a crucial role in programmed cell death. We tried to evaluate how far the status of pro or anti apoptotic p53, Bax, caspase-3, caspase-9, Bcl-$_{XL}$ and Bcl-2 is responsible for governing the susceptibility towards ENU induced tumor development in Swiss and Balb/c F1 mice in our study.

ENU exposure resulted into an upregulation of mutp53, Bcl-$_{XL}$ and Bcl-2 in F1 mice (Figure-3). Up regulation in mRNA of mutp53, Bcl-$_{XL}$ and Bcl-2 was 29, 31 and 31% in Swiss F1 mice while this expression for respective genes was increased to 38, 82 and 62% in Balb/c F1 mice as compared to control. In presence of 2% IP6, upregulation of mRNA of the respective genes was reduced to 8, 7, and 8% in Swiss F1 and 0, 59 and 15% in Balb/c F1 mice with respect to control (Figure 3-I). At the protein level, upregulation of mut p53, Bcl-$_{XL}$ and Bcl-2, was 67, 44, and 61% in Swiss F1 and this upregulation increased to 76, 195 and 126% in Balb/c F1 mice from the ENU exposed mothers as compared to control. In the presence of 2% IP6, this upregulation was reduced to 38, 6 and 19% in Swiss F1 mice and 4, 25 and 52% in Balb/c F1 mice with respect to control (Figure 3-III).

Pro-apoptotic genes Bax, caspase-3 and csapase-9 were down regulated in F1 generation from the ENU exposed mothers. ENU caused decrease in the levels of Bax, caspase-3 or caspase-9 was 34, 28 or 24% at mRNA and 17, 38 or 27% at protein level in Swiss F1 mice. Whereas, this down regulation for the respective genes was 27, 20 or 47% at mRNA and 28, 42 or 40% at the protein level in Balb/c F1 mice as compared to control. The presence of IP6 elevated the expression of respective genes by 26, 4 or 15% at mRNA and 8, 21 or 0% at protein level in Swiss F1 mice. Whereas, this upregulation was 6, 46 or 11% at mRNA and 6, 14 or 16 % at protein level in Balb/c F1 mice as compared to control (Figure 4- I, III).

Bax/Bcl-2 Ratio at Protein and mRNA Level

An increase in the Bax/Bcl-2 ratio corresponds with the onset of apoptosis. We observed that ENU exposure resulted in a decrease in Bax/Bcl-2 ratios, both at the mRNA and protein levels. The decrease was 51 and 50% in Swiss F1 mice and 55 and 57 % in Balb/c F1 mice as compared to control. Presence of IP6 tried to attenuate this decrease and showed only 33, 17% decrease in Swiss F1 and 12 and 28 % decrease in Balb/c F1 mice at mRNA and protein level as compared to control (Figure 5- I, II).

Enzyme Activity of Caspase-3 and Caspase-9

Having shown the expression of caspase-3 and caspase-9 genes, we tried to show their functionality in terms of the enzymatic activity of caspase-3 and caspase-9 in both Swiss and Balb/c F1 mice from the ENU exposed mothers. The enzyme activity of caspase-3 and caspase-9 showed an inhibition of 26 and 43% in Swiss F1 mice and 63 and 67% in Balb/c F1

as compared to control. ENU caused inhibition of the activity of respective enzymes in the presence of IP6 was reduced and showed only 11 and 25% in Swiss F1 while 25 and 4% in Balb/c F1 as compared to control (Figure 5-III, IV) .

DNA Breakdown as Detected by TUNEL Assay

In order to show the status of apoptosis, we evaluated the DNA breakdown by doing the TUNEL assay (Figure 5-V). There was no DNA fragmentation in either of Swiss and Balb/c F1 from the ENU exposed mothers. DNA fragmentation, as indicated by the intensity of the brown stain, appeared to be increased in the presence of IP6 (Arrow in figure 5-V) both in Swiss and Balb/c F1 mice. However, the intensity of the brown stain in the stained cells indicating DNA fragmentation and thus, the increased incidence of apoptosis in presence of the IP6, appeared to be same, in both Swiss and Balb/c F1 mice. This suggests that the apoptotic events are altered in F1 mice irrespective of the development of tumors.

DISCUSSION

We hypothesize that the risks associated with *in utero* exposure to environmental carcinogens could be due to the alterations at the molecular level. We tried to demonstrate the molecular alterations with respect to susceptibility towards the effects of tumorigen in both Swiss and Balb/c F1 mice from the mothers exposed to ENU on the 17^{th} day of gestation as transplacental induction of lung tumors in offspring is affected by the day of gestation for carcinogen treatment [3]. ENU, a direct acting carcinogen, did not result tumors on the lung surface, but caused distinct hispathological changes in terms of lymphocytic infiltration in Swiss F1 mice. But over the same time period, well defined tumors appeared on the lung surface and adenomas, were observed in Balb/c F1 mice. These alterations were sensitive towards the presence of antitumor agent, IP6 in both the strains. In the presence of IP6, lymphocytic infiltration was attenuated in Swiss F1 mice and significant reduction in the number and size of lung tumors was observed in Balb/c mice. These results are supported by the earlier observations where we had shown the appearance and prevention of lymphocytic infiltration and hyperplasia in mouse lungs [34].

The differential tumorigenic effect provided the basis for further evaluation of the molecular modulations which might account for the differential susceptibility in these strains [36] as well as the modulatory effects of IP6 towards the ENU exposure [34] in F1 mice. Cyclin D1 and nuclear factor (Nf-κβ) play a major role in lung tumorigenesis by regulating several pathways involved in tumor development [10]. Nf-κβp50 and cyclin D1 were up regulated in both Swiss and Balb/c F1 mice, but Nf-κβ and cyclin D1 appeared to be more responsive in

Balb/c F1 mice as compared to Swiss F1 mice. COX-2 plays important role in the inflammatory process and is over expressed both in human and mouse models. Our results on the stratus of COX-2 expression are in agreement with the published reports showing over expression of COX-2 in tumorigenesis. However, we could not observe any difference in COX-2 gene expression in Swiss and Balb/c F1 mice.

Apoptosis is inhibited or slowed down during tumor development and its restoration is mediated by activation of caspase-3 and caspase-9 [37] .We also showed the downregulation of the expression as well as the functional activities of pro-apoptotic caspase-3 and caspase-9 gene in response to ENU during transplacental lung tumor development in Balb/c F1 mice and also in Swiss F1 mice where tumors did not develop. This suggests that the apoptotic events are disrupted and could lead to the reduction of apoptosis in predisposed conditions irrespective of the appearance of tumors.

We substantiated the hypothesis that apoptotic events play an important role towards the tumorigenic susceptibility by analyzing Bcl-2 family of proteins. IP6 induced apoptosis was associated with the upregulation of Bax and down regulation of Bcl-2 leading to caspase-3, caspase-9 activation and DNA fragmentation (TUNEL) result in the induction of apoptosis in p53 dependent pathway [38]. The high level of p53 increased the ratio of Bax/ Bcl-2 and resulted the induction of apoptosis [39]. Likewise, the inverse effect on Bax and Bcl-2 expressions in F1 mice from the ENU exposed mothers was attenuated in the presence of IP6. Reduction in the Bax: Bcl-2 ratio from the ENU exposed population appeared to be same in

Balb/c or Swiss F1 mice and similar effects of IP6 were observed in both the strains. This suggests the importance of the apoptotic events irrespective to the appearance of tumors and tumorigenesis involves other associated molecular modulations.

Since, IP6 inhibited the tumor development and restored the altered apoptotic events, these results imply that IP6 might be exerting its chemopreventive effects by up regulating the apoptotic pathways in the F1 generation. IP6 induced apoptosis in terms of the status of p53, Bcl-$_{XL,}$ Bax/Bcl-2 ratio, caspase-3, and caspase-9 resulted in the restriction of ENU induced transplacental lung tumorigenesis [24]. In addition, the decrease in expression status of COX-2, Nf-κβp50 and cyclin D1 could also be the basis of chemopreventive effects of IP6 during transplacental lung tumorigenesis in F1 mice as suggested earlier [10, 11].

The results suggest that molecular changes occurs even before the onset of tumors .Further, the degree of gene expression may be associated with the differential susceptibility to the development of lung tumors in the F1 generation from the mothers predisposed to tumorigen [40]. The genes involved in cell proliferation, chronic inflammation and apoptosis were more responsive toward the ENU induced transplacental lung tumorigenesis in Balb/c F1 as compared to Swiss F1. The strain-dependent differences in these altered genes might have subsequently created microenvironment to play vital role in transplacental lung tumor development [1]. Therefore, we could say that Balb/c F1 mice are more sensitive towards the lung tumor induction, while Swiss mice are less sensitive at the given time period and also imply that the chemopreventive effects of IP6 appeared to be mediated by the regulation of

cyclin D1, Nf-κβ, COX-2, Bcl-2, Bcl-$_{XL}$, Bax, caspase-3, caspase-9, and p53 genes in ENU induced transplacental lung tumorigenesis. Our data would be useful in exploring the molecular alterations for the differential susceptibility for the tumor development and its control.

CONFLICT OF INTERESTS

The authors report no conflicts of interest.

FUNDING

This work was supported by the Indian Council of Medical Research and University Grants Commission, New Delhi. India

ACKNOWLEDGEMENTS

The authors would like to thank Director, CSIR-Indian Institute of Toxicology Research, Lucknow for providing the facilities and Ms. Pratima Uppadhyay for her help in hisopathological work.

REFERENCES

[1] Gordon T, Bosland M**.** Strain-dependent differences in susceptibility to lung cancer in inbred mice exposed to mainstream cigarette smoke. Cancer Lett 2009; 275:213–220.

[2] Maritz GS, Rayise SS. Effect of maternal nicotine exposure on neonatal rat lung development: protective effect of maternal ascorbic acid supplementation. Experimental Lung Research 2011; 37:57–65.

[3] Castro DJ, Yu Zhen, Lohr CV, Pereira CB. Chemoprevention of dibenzo[a,l]pyrene transplacental carcinogenesis in mice born to mothers administered green tea: primary role of caffeine. Carcinogenesis 2008; 29:1581–1586.

[4] Capilla-Gonzalez V, Gil-Perotin S, Ferragud A, Bonet-Ponce L, Canales JJ, Garcia-Verdugo JM. Exposure to N-ethyl-N-nitrosourea in adult mice alters structural and functional integrity of neurogenic sites. PloS one 2012; 7 (1): e29891.

[5] Rice JM. Transplacental carcinogenesis in mice by 1-ethyl- 1-nitrosourea. Ann. NY Acad. Sci.1969; 163:813-827.

[6] Campos KKD, Dourado VA, Diniz MF, Bezerra FS, Lima WG. Exposure to cigarette smoke during pregnancy causes redox imbalance and histological damage in lung tissue of neonatal mice. Experimental Lung Research 2014; 40: 164–171.

[7] Slikker W, Mei N, Chen T. N-ethyl-N-nitrosourea (ENU) increased brain mutations in prenatal and neonatal mice but not in the adults. Toxicol. Sci 2004; 81: 112-120.

[8] Malkinson AM. Primary lung tumors in mice as an aid for understanding, preventing, and treating human adenocarcinoma of the lung. Lung Cancer 2001; 32:265–279.

[9] Malkinson AM. Molecular comparison of human and mouse pulmonary adenocarcinomas. Experimental Lung Research 1998; 24:541–555.

[10] John S, Alao P. The regulation of cyclin D1 degradation roles in cancer development and the potential for therapeutic invention. Mol. Cancer 2007; 2:6-24.

[11] Pandey M, Gupta KP. Involvement of STAT3, NF-κB and associate downstream molecules before and after the onset of urethane induced lung tumors in mouse. Environ. Toxicol. Applied Pharmacol 2012; 34:502-511.

[12] Dolcet X, Llobet D, Pallares J, Matias-Guiu X. Nfκβ in development and progression of human cancer, Virchows Archiv 2005; 446:475–482.

[13] Nishikori M. Classical and alternative Nfκβ activation pathways and their roles in lymphoid Malignancies. J. Clin. Exp. Hematop 2005; 45:15-24.

[14] Hull MA. Cyclooxygenase-2: How good is it as a target for cancer chemoprevention. Eur. J. Cancer 2005; 1:1854–1863.

[15] Hida T, Yatabe Y. Increased expression of cyclooxygenase 2 occurs frequently in human lung cancers, specifically in adenocarcinomas. Cancer Res 1998; 58:3761–3764.

[16] Das T, Sa G, Sinha P, Ray PK. Induction of cell proliferation and apoptosis: dependence on the dose of the inducer. Biochem. Biophys. Res. Commun 1999; 260:105–110.

[17] Basu A, Haldar S. The relationship between Bcl2, Bax and p53: consequences for cell cycle progression and cell death. Mol. Hum. Repro 1998; 4:1099–1109.

[18] Singh N, Sarkar J, Sashidhara KV, Ali S, Sinha S. Anti-tumour activity of a novel coumarin–chalcone hybrid is mediated through intrinsic apoptotic pathway by inducing PUMA and altering Bax/Bcl-2 ratio. Apoptosis 2014; 19:1017–1028.

[19] Bickers DR, Athar M. Novel approaches to chemoprevention of skin cancer. J. Dermatol 2000; 27:691–695.

[20] Shafie NH, Esa NM, Ithnin H, Norazalina S, Pandurangan AK. Pro-Apoptotic Effect of Rice Bran Inositol Hexaphosphate (IP6) on HT-29 Colorectal Cancer Cells. Int. J. Mol. Sci. 2013; 14: 23545-23558.

[21] Miyashita T et al. Tumor suppressor p53 is a regulator of bcl-2 and bax gene expression in vitro and in vivo. Oncogene 1994; 9:1799–1805.

[22] Shamsuddin AM, Vucenik I. Mammary tumor inhibition by IP6: a review. Anticancer Res 1999; 19:3671–3674.

[23] Shamsuddin AM, Vucenik I, Cole KE. IP6: a novel anticancer agent. Life Sci 1997; 61:343 354.

[24] Shamsuddin AM, Yang GY, Vucenik I. Novel anticancer functions of IP6: growth inhibition and differentiation of human mammary cancer cell lines in vitro. Anticancer Res 1996; 16:3287–3292.

[25] Singh J, Gupta KP. Inositol hexaphosphate induces apoptosis by coordinative modulation of p53, Bcl2, and sequential activation of caspases in 7,12 imethylbenz[a]anthracene-exposed mouse epidermis. J. Environ. Pathol. Toxicol. Oncol 2008; 27:209–217.

[26] Vucenik I et al. Antiangiogenic activity of inositol hexaphosphate (IP6). Carcinogenesis 2004; 25:2115–2123.

[27] Norazalina WM, Hairuszah I, Norashareena MS. Anticarcinogenic efficacy of phytic acid extracted from rice bran on azoxymethane-induced colon carcinogenesis in rats. Exp. Toxicol. Pathol 2010;62:259–268

[28] Schroterova L, Haskova P, Rudolf E, Cervinka M. Effect of phytic acid and inositol on the proliferation and apoptosis of cells derived from colorectal carcinoma. Oncol. Rep. 2010; 23: 787–793

[29] Karpel M, Wawszczyk J, Hollek A, Weglarz L. Induction of the expression of genes encoding TGF-beta isoforms and their receptors by inositol hexaphosphate in human colon cancer cells. Acta. Pol. Pharm 2013;70(2):357-63

[30] Vucenik I, Yang GY, Shamsuddin AM. Comparison of pure inositol hexaphosphate and high-bran diet in the prevention of DMBA-induced rat mammary carcinogenesis. Nutr. Cancer 1997; 28:7–13.

[31] Singh RP et al. In vivo suppression of hormone-refractory prostate cancer growth by inositol hexaphosphate: induction of insulin-like growth factor binding protein-3 and inhibition of vascular endothelial growth factor. Clin. Cancer Res 2004; 10:244–250.

[32] Raina K, Rajamanickam S, Singh RP, Agarwal R. Chemopreventive efficacy of inositol hexaphosphate against prostate tumor growth and progression in TRAMP mice. Clin. Cancer Res 2008; 14:3177–3184.

[33] Bharti AC, Donato N, Singh S, Aggarwal BB. Curcumin (diferuloylmethane) down-regulates the constitutive activation of nuclear factor-kappa B and IkappaB alpha

kinase in human multitude myeloma cells, leading to suppression of proliferation and induction of apoptosis. Blood 2003; 101:1053-1062.

[34] Pandey M, Gupta KP. Epigenetics, an early event in the modulation of gene expression by inositol hexaphosphate in ethylnitrosourea exposed mouse lungs. Nutr. Cancer 2011; 63:89-99.

[35] Thakur P, Sanyal SN. Chemopreventive Role of Preferential COX-2 Inhibitor Diclofenac in 9, 10- Dimethybenz(a)anthracene Induced Experimental Lung Carcinogenesis. Am. J. Biomed. Sci 2010; 2:275-288.

[36] Peter JA. Strain-specific tumorigenesis in mouse skin induced by the carcinogen 15,16-dihydro-11-methylcyclopenta[a]phenanthren-17-one and its relation to dna adduct formation and persistence. Cancer Research 1983;43: 2261-2266.

[37] Chang HC , Weng CF. Cyclooxygenase-2 level and culture conditions influence NS398-induced apoptosis and caspase activation in lung cancer cells, Oncol. Res 2001; 8:1321–1325.

[38] Agarwal C et al. Inositol hexaphosphate inhibits growth and induces G1 arrest and apoptotic death of androgen-dependent human prostate carcinoma LNCaP cells. Neoplasia 2004; 6:646–659.

[39] Katiyar SK, Roy AM, Baliga MS. Silymarin induces apoptosis primarily through a p53-dependent pathway involving Bcl-2/Bax, cytochrome c release, and caspase activation. Mol. Cancer. Ther 2005; 4:207-16.

[40] Miller MS, Gressani KM, Leone-Kabler S, Townsend AJ, Malkinson AM, O'Sullivan MG. Differential sensitivity to lung tumorigenesis following transplacental exposure of mice to polycyclic hydrocarbons, heterocyclic amines, and lung tumor promoters. Experimental Lung Research 2000; 26:709 –730.

TABLE 1. Experiment Design and Treatment Schedule

Treatment on the 17th day of gestation.	**Groups**	**Number of pups (N)**		**Weaning (Days)**	**Treatment (After weaning)**
		Swiss	**Balb/c**		
50mM citrate, pH 6.0 (i.p.), Once. (No. of pregnant mice =6)	1	14	15	24	Normal drinking water.
	2	14	15	24	2% IP6 in drinking water.
ENU (i.p.) 40 mg/kg.bwt in 50mM citrate, pH 6.0, Once. (No. of pregnant mice =6)	3	15	15	24	Normal drinking water
	4	14	18	24	2% IP6 in drinking water.

TABLE 2. Nucleotide Sequences of Primers and PCR Product Size for RT-PCR

Gene	Nucleotide Sequences	Annealing Temperature ^{0}(C)	Product Size (bp)
COX-2	F 5'-GTGGAAAAACCTCGTCCAGA-3' R 5'-TGATGGTGGCTGTTTTGGTA-3'	60	256
Cyclin D1	F 5'TGTTCGTGGCCTCTAAGATGAAG-3' R 5'AGGTTCCACTTGAGCTTGTTCAC-3'	58	136
mut p53	F 5'-ATGACTGCCATGGAGGAGTC-3' R 5'-CTCGGGTGGCTCATAAGGTA-3'	58	663
Nf-κβ p50	F 5'GCACAGACGGTGTCTAGCAA-3' R 5'GCGGAGGGACAGCAGTAACA-3'	58	131
Bcl-2	F 5'- AGCCCGTGTTTGTAATGGAG-3' R 5'- CACAGCCTTGATTTTGCTGA-3'	58	476
Bcl-$_{XL}$	F 5'-AGGCAGGCGATGAGTTTGAAC-3' R 5'-GAACCACACCAGCCACAGTCA-3'	61	399
Bax	F 5'-TGTTTGCTGATGGCAACTTC-3' R 5'-GATCAGCTCGGGCACTTTAG-3'	58	104
caspase-3	F 5'-AGGGGTCATTTATGGGACAAA-3' R 5'-TACACGGGATCTGTTTCTTTG-3'	57	127
caspase-9	F 5' -CAGGCCCGTGGACATTGGTT-3' R 5'-CAGCCGCTCCCGTTGAAGATA-3'	62	438
β-actin	F 5'-TGTGATGGTGGGAATGGGTCAG-3' R 5'-TTTGATGTCACGCACGATTTCC-3'	60	514

FIGURE LEGENDS

FIGURE- 1. Evaluation of ENU induced development of transplacental lung tumors in both Swiss and Balb/c F1 mice at the end of three months. Gross (I) examination of tumors in tumor bearing mice and microscopic (II, III) examination of lung of both Swiss and Balb/c F1 mice. Lymphocytic infiltration in Swiss F1 and tumors in Balb/c F1 is shown by the arrows. Quantitative analysis of tumor status and tumor area in Balb/c F1 mice is shown by the histograms in (I, III). Bars represent mean value +/- SD. $^{\dagger}P<0.05$, $^{\dagger\dagger}P<0.01$ .Magnification-40X.

FIGURE - 2. Evaluation of proliferation, inflammation markers in F1 Swiss and Balb/c mice. Analysis of cyclin-D1, NF-κβ p50 and COX-2 mRNA by RT-PCR (I) and protein by western blotting (III) is shown for both Swiss and Balb/c F1 mice. Quantitative analysis is shown by histrograms (II, IV). Three individual samples were analyzed for the expression of genes and were subjected to statistical analysis. Bars represent mean value +/- SD. $^{*,\dagger}P<0.05$; **,†† $P<0.01$. *,**, compared with control and †,††, compared with ENU. Swiss, Balb/c

FIGURE- 3. Analysis of mut p53, Bcl-$_{XL}$ and Bcl-2 mRNA by RT-PCR (I) and protein by western blotting (III) are shown for both Swiss and Balb/c F1 mice. Quantitative analysis is shown by the histograms (II, IV). Three individual samples were analyzed for the expression of genes and were subjected to statistical analysis. Bars represent mean value +/- SD. $^{*,\dagger}P<0.05$; **,†† $P<0.01$. *,**, compared with control and †,††, compared with ENU.

Swiss, Balb/c

FIGURE - 4. Analysis of Bax, caspase-3 and caspase-9 mRNA by RT-PCR (I) and protein by western blotting (III) is shown for both Swiss and Balb/c F1 mice. Quantitative analysis is shown by the histograms (II, IV). Three individual samples were analyzed for the expression of genes and were subjected to statistical analysis. Bars represent mean value +/- SD. $^{*,\dagger}P<0.05$; †† $P<0.01$. * compared with control and †,††compared with ENU.

FIGURE - 5. Assessment of apoptotic events in Swiss and Balb/c F1 mice. Quantitative analysis of the Bax/Bcl-2 ratio at mRNA and protein level in both Swiss and Balb/c F1 mice is shown by the histograms (I, II). Three individual samples were analyzed for the expression of genes. Quantitative analysis of caspase-3 and caspase-9 enzyme activity is shown by histograms (III, IV). Three individual samples were analyzed in triplicate for the enzyme assay and were subjected to statistical analysis. Bars represent mean value +/- SD. $^{*,\dagger}P<0.05$; **,†† $P<0.01$. *,** compared with control and †,††compared with ENU.

Evaluation of apoptosis by TUNEL assay in lung tissue sections of both Swiss and Balb/c F1 mice is shown in (Figure 5-V). Fragmented DNA in apoptotic cells is stained brown with DAB and is shown by arrows. Magnification - 100X.

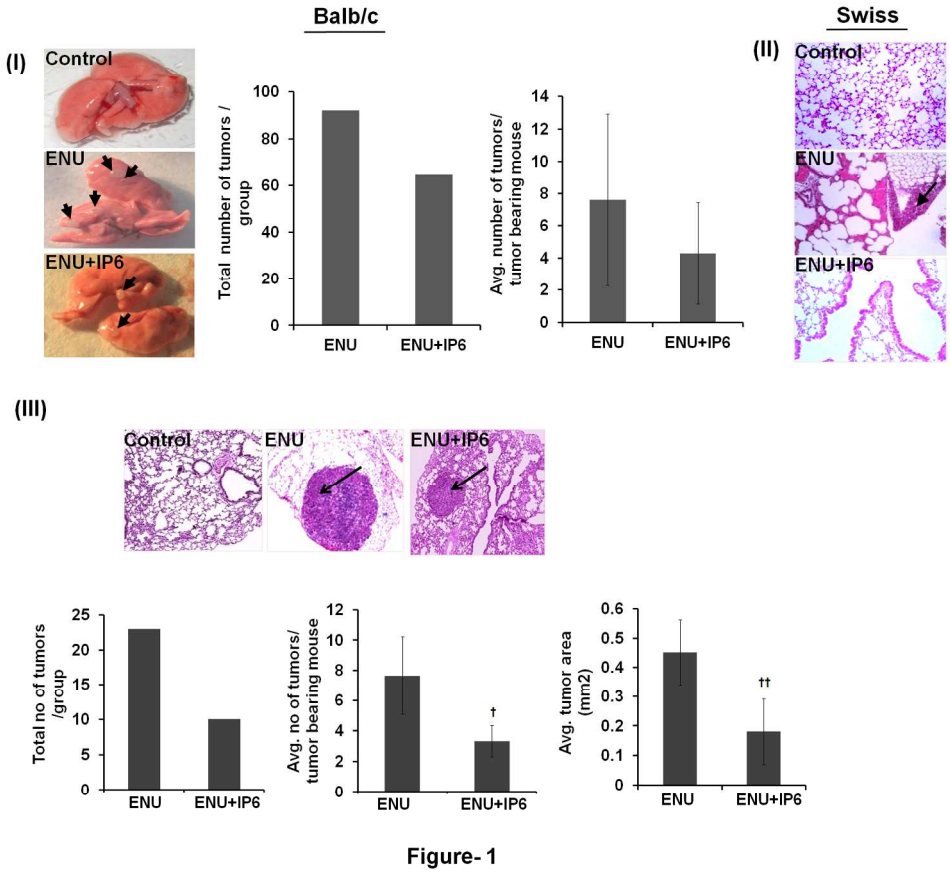

Figure- 1

Evaluation of ENU induced development of transplacental lung tumors in both Swiss and Balb/c F1 mice.
519x479mm (300 x 300 DPI)

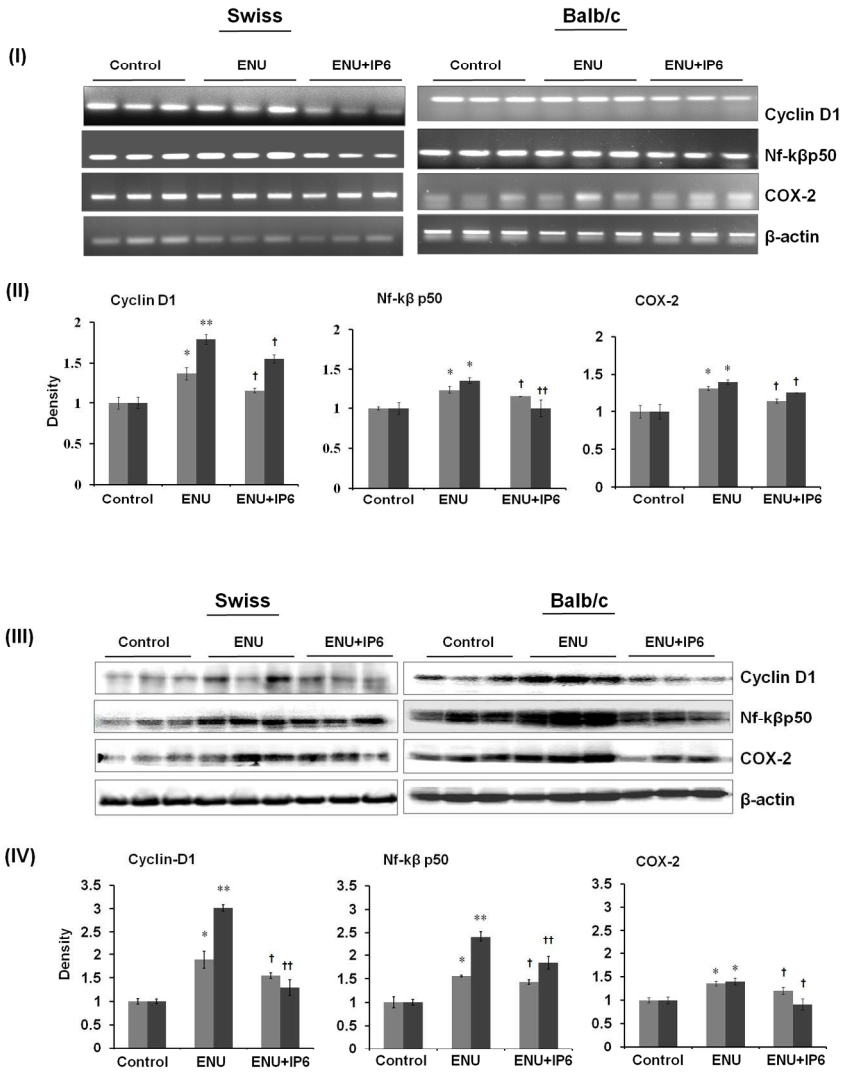

Figure- 2

Evaluation of proliferation, inflammation markers in F1 Swiss and Balb/c mice.
224x278mm (300 x 300 DPI)

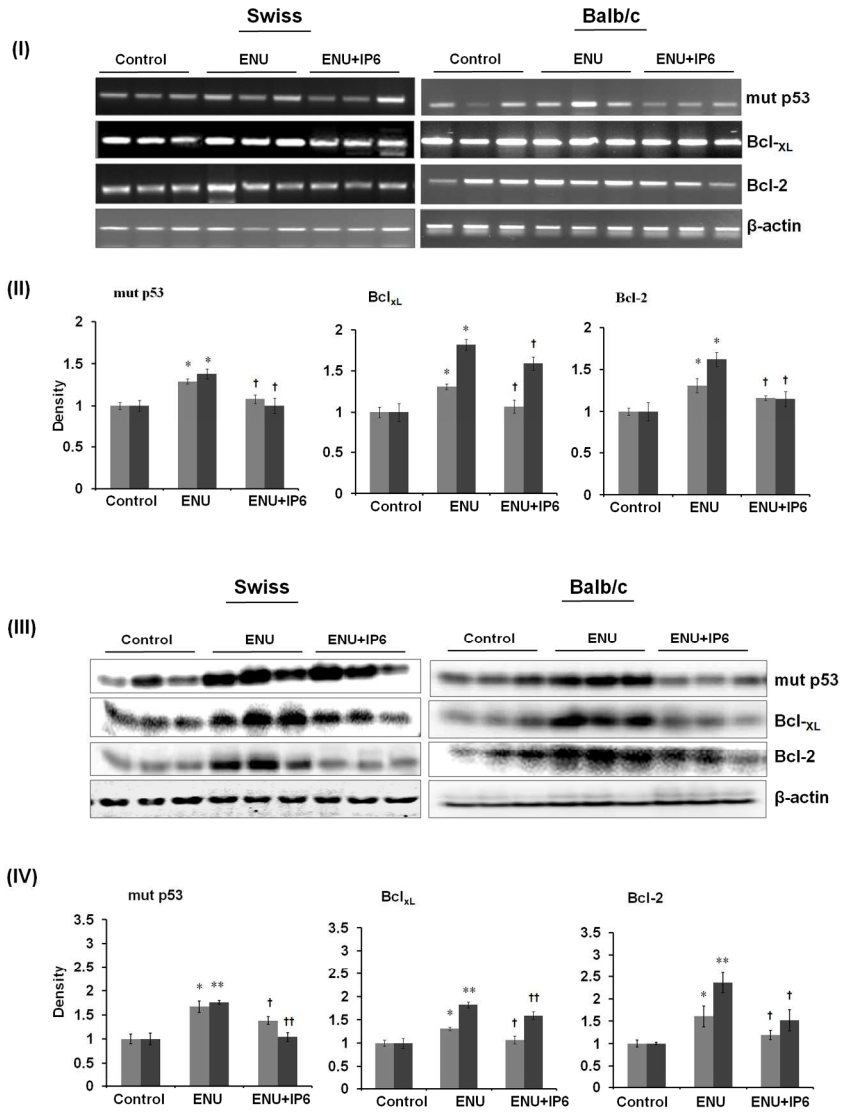

Figure- 3

Analysis of mut p53, Bcl-XL and Bcl-2 mRNA by RT-PCR (I) and protein by western blotting (III) are shown for both Swiss and Balb/c F1 mice.
224x278mm (300 x 300 DPI)

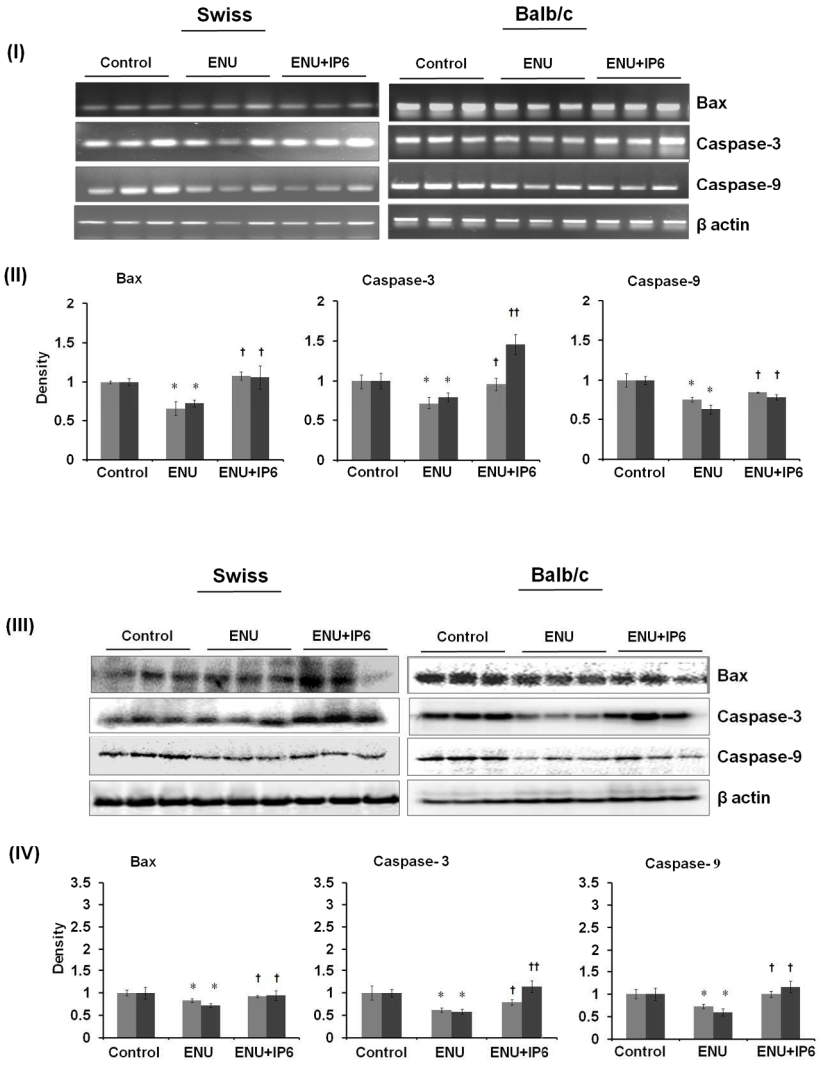

Figure- 4

224x278mm (300 x 300 DPI)

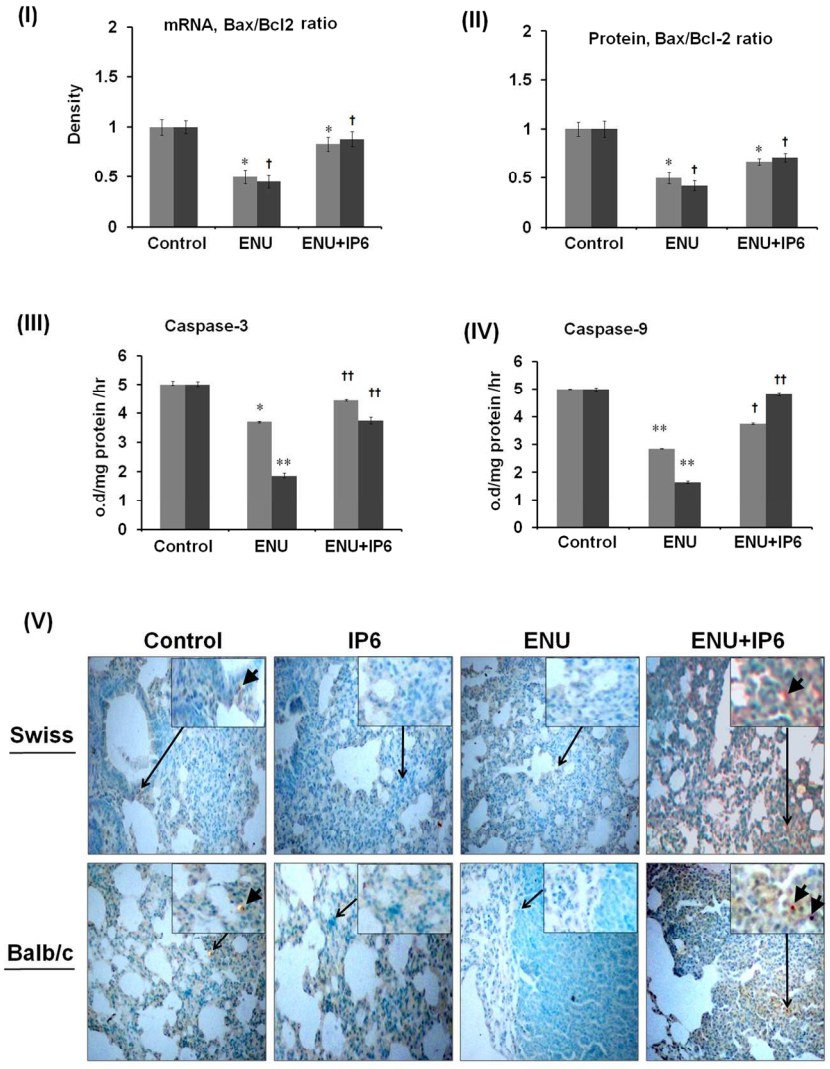

Figure- 5

Assessment of apoptotic events in Swiss and Balb/c F1 mice.
148x195mm (300 x 300 DPI)